

Research Article

Kinematic Modeling and Simulation of Eleven-Links Biped Robot With Arms

Nima Sina^{1,*}, Alireza Ariaei², Javad Jafari Fesharaki¹, Masoud Afrand¹

(1) Department of Mechanical Engineering, Najafabad Branch, Islamic Azad University, Isfahan, Iran.

(2) Department of Mechanical Engineering, University of Isfahan, Isfahan, Iran.



Australian International Academic Centre, Australia

doi:10.7575/aiac.ijaep.v.2n.2p.1

Article history:

Received 18 June 2014
 Reviewed 10 September 2014
 Revised 21 October 2014
 Accepted 27 October 2014
 Published 15 November 2014

Abstract. Gait generation for humanoids and humanoid walking has been subject of many researches in robotics. This paper focuses on mathematical simulation of biped robots and investigating walking stability regarding zero moment point (ZMP) criteria; it also proposes a simple algorithm for humanoid walking with more links such as arms and forearms using proper parameters. Raising the number of links, the number of effective parameter instability grows rapidly and leads to be complicated and time consuming equations. In order to tackle the issue, a new method, step by step ZMP calculating is used. It can be seen that robot walking pattern with the swinging arm and forearm is like a human walking patterns. Besides, it is understood that a robot with arms has more stability in comparison with the robot without arms. Moreover, it is concluded that robot with forearms has more stability in comparison with the robot with arms.

Keywords: biped robot, ZMP, arm, trajectory, simulation, modeling, spline.

1 Introduction

In recent years, many researchers have worked on humanoid robots to perform tasks that humans cannot make^[1]. A basic topic in legged walking machines is the gait stability of legged locomotion. Some researches are performed on mathematical modeling a biped robot^[2,3]. Vukobratovic et al.^[2] worked on dynamic stability of legged machines. Yagi and Lumelsky^[3] used sensors to plan the motion of a biped robot. They studied a number of stable walking patterns. Using multi objective particle swarm optimization algorithm, Mahmood-abadi et al.^[4] studied on optimal control of a biped robot. Bououden and Abdessemed^[5] investigated on control of a biped robot. They considered suitable geometrical conditions to transform the nonlinear systems to normal form and proposed a strategy for controller design of a walking robot. Based on the system of T-S Fuzzy, Farzaneh et al. determined an analytical function and presented a new method for trajectory generation of a seven-link biped robot^[6].

Aoustin and Hamon^[7] worked on a four-bar linkage biped robot. They simulated the dynamic of a biped robot with four-bar linkage knees. The numerical results from their research show that the four-bar linkage simulation is a good way to simulate the robots.

McGeer^[8] investigated the passive walking with knees. Passive walking is a phenomenon used for bipeds having straight legs. Some researchers used static con-

cept of walking^[9], and others used the dynamic concept for walking^[10] to calculate the pattern for walking. Zheng and Shen^[9] presented a plan to enable the SD-2 biped robot to climb a ramp surface. They showed that the proposed mechanism can be extended to quasi-dynamic and dynamic gaits. Dasgupta and Nakamura^[10] studied the human/humanoid locomotion system and a method for adaptation of the human motion capture data for driving a robot like humans.

On the other hand, Grizzle et al.^[11] modeled the walking control of a three-dimensional bipedal robot. Besides, Siswoyo Jo and Mir-Nasiri^[12] simulated and modeled the dynamic walking of a bipedal robot. They used a minimum degree of freedom for walking and presented a new method for balancing and sensing for robot. Moreover, Juang^[13] presented a learning scheme to generate robotic locomotion on different sloping surfaces. And finally, Sabourin and Bruneau^[14] studied a method for dynamic control of an under-actuated robot.

In 2007, Wu et al.^[15] worked on a system for trajectory tracking control of a biped robot using neural network. However, before them, in a related study, Capi et al.^[16] have been also presented a scheme for designing a learned inverse dynamics of a robot with two legs by using neural network algorithm in 2003.

Kajita et al.^[17] developed a biped which can jump and run. Previously, in another work, Silva and Machado^[18] studied the analysis of biped robot locomotion systems, focusing on the problem of energy efficiency. However, Cardenas-Maciel et al.^[19] worked on designation the walking motion for a biped robot using the genetic algo-

*Corresponding author: N. Sina

☎: +98 910 314 3358

✉: nimasina_matlab@yahoo.com

rithm as a method for their work, in 2011. They used a three degree of freedom robot as a case study for their designation. In the same year, Pinto and Santos [20] modeled two-legged robots like animals. Before them, Huang et al. [21] have formulated parameter constraints of the robot’s motion and proposed different types of motion on the ground.

Based on reviewed studies, gait generation includes a variety of different methods. However, plan a gait for a humanoid robot with more than seven-links is the main problem which is still existing in most of these surveyed methods. Therefore, a new proposed method for covering this problem should not be complicated.

First of all, based on the method of Mousavi and Bagheri [22], this manuscript presents a simulation method for a biped robot with a seven-links biped robot, without arms; and by iteration obtains some effective parameters in the ZMP. After that, by adding another four-links as arms and forearms, the simulation performs using parameters gained from the seven-links biped robot. By examination of new effective parameters which are related to the new four-links, the best values of them will be selected for gate generation in this new robot. The considerable benefit of applying this technique is that it is not required to use huge iteration; and as a result, the new ZMP can be calculated quickly.

2 Kinematic Modeling of the Biped Robot, Based on the Calculation of Mousavi and Bagheri

An effective method for walking is presented using inverse kinematics. Polynomials and the spline functions were used because of the reason that these are good functions for specifying trajectory of each joint, since splines are differentiable and easy for evaluating. Respecting to the break points (i.e. step length and geometrical conditions), the ankle trajectory is generated. By using $n + 1$, different points are becoming more suitable to calculate coefficients of a polynomial in order of n and as a result, this polynomial would be unique. The lengths of links are known. Therefore, the position of links during walking can be found by applying the geometrical relations. It is necessary to introduce some of utilized parameters and assumptions in modeling of this biped robot. These parameters are *hip* and *foot* parameters, which are explained as follows.

2.1 Hip Parameters in Sagittal Plane

Hip parameters include vertical and horizontal displacements (z_h, x_h) , which are shown in Fig. 1. These parameters are used in the trajectory of the hip. During inverse kinematic these two parameters are needed to be calculated, which are horizontal and vertical positions of the hip.

2.2 Foot Parameters

Foot includes parameters such as horizontal displacement of ankle (x_a) , vertical displacement of ankle (z_a) , time of total traveling which is single and double support phase (T_c) , time of double support phase (T_d) , the time that ankle joint reaches maximum height (T_m) , step numbers (k) , Maximum height on ankle joint (H_{ao}) , the horizontal distance between start point and ankle joint for maximum height of ankle joint (L_{ao}) , length of half

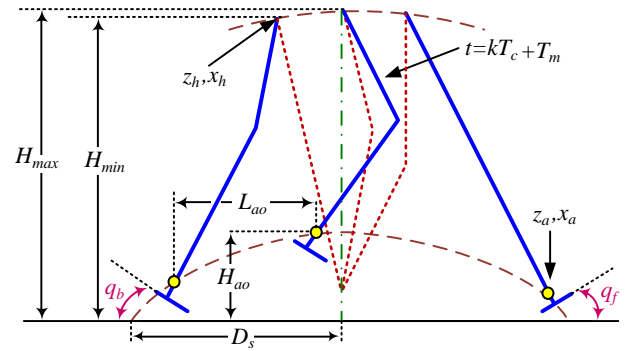


Fig. 1. Biped robot sagittal configuration [22]

a step D_s , angles of foot lift and contact with the level ground $(q_b$ and $q_f)$; and the angles of ground initial terrain $(q_{gs}$ and $q_{gf})$. These parameters are used to generate ankle and foot trajectory. Some of these parameters are also illustrated in Fig. 1.

Additionally, there are two extra important parameters which are named x_{sd} and x_{ed} . The parameter x_{sd} is the distance between the ankle joint and hip of the support leg, horizontally, in the beginning of the double supports; and the parameter x_{ed} is the distance between the hip and ankle joints, horizontally, at the end of the double support phase. These parameters are shown in Fig. 2.

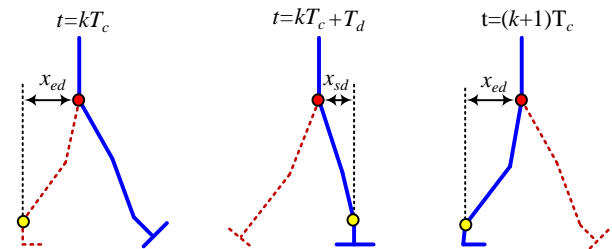


Fig. 2. Parameters of hip (x_{ed}, x_{sd}) [22]

2.3 Foot Configuration

Foot plays an important role in walking. In this case, foot parameters are shown in Fig. 3. This configuration is similar to the humans foot. During a real walking process foot and ankle should be concerned. Therefore, in an ankle trajectory, this configuration is also important.

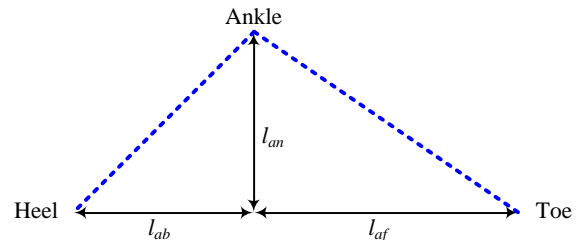


Fig. 3. Foot configuration [22]

In Fig. 3, l_{ab} is the distance between the ankle and the heel, l_{af} is the distance between the ankle and the toe; and l_{an} is the height of the ankle.

2.4 Ankle Trajectory

When the foot is traveling, considering the geometrical constraints and avoiding collisions, it is important to consider (1a) and (1b) conditions for angular position and

velocity of the ankle joints.

$$\theta_a(t) = \begin{cases} -q_{gs} & t = kT_c \\ -q_b & t = kT_c + T_d \\ q_f & t = (k+1)T_c \\ q_{gf} & t = (k+1)T_c + T_d \end{cases} \quad (1a)$$

$$\dot{\theta}_a(t) = \begin{cases} 0 & t = kT_c \\ 0 & t = (k+1)T_c + T_d \end{cases} \quad (1b)$$

Horizontal and vertical displacement of swing legs during walking is calculated from (2a) and (2b).

$$x_a(t) = \begin{cases} kD_s & t = kT_c \\ kD_s + l_{an} \sin(q_b) \cdots \\ \quad + l_{af} (1 - \cos(q_b)) & t = kT_c + T_d \\ kD_s + l_{ao} & t = kT_c + T_m \\ (k+2)D_s \cdots & t = (k+1)T_c \\ -l_{an} \sin(q_f) \cdots \\ -l_{ab} (1 - \cos(q_f)) & t = (k+1)T_c + T_d \\ (k+2)D_s & t = (k+1)T_c + T_d \end{cases} \quad (2a)$$

$$z_a(t) = \begin{cases} h_{gs} + l_{an} & t = kT_c \\ h_{gs} + l_{af} \sin(q_b) \cdots \\ \quad + l_{an} (1 - \cos(q_b)) & t = kT_c + T_d \\ H_{ao} & t = kT_c + T_m \\ h_{ge} + l_{ab} \sin(q_f) \cdots \\ \quad + l_{an} (1 - \cos(q_f)) & t = (k+1)T_c \\ h_{ge} + l_{an} & t = (k+1)T_c + T_d \end{cases} \quad (2b)$$

where l_{ao} is the horizontal distance traveled between the ankle joint and the start point when the ankle joint has its maximum height. h_{gs} and h_{ge} are the height of ground initial terrain. Both of these two parameters are zero because of the lack of ground's inclination. z_a is the vertical position of the ankle.

The horizontal and the vertical velocity of the ankle in landing are zero and therefore,

$$\dot{x}_a(t) = \begin{cases} 0 & t = kT_c \\ 0 & t = (k+1)T_c + T_d \end{cases} \quad (3a)$$

$$\dot{z}_a(t) = \begin{cases} 0 & t = kT_c \\ 0 & t = (k+1)T_c + T_d \end{cases} \quad (3b)$$

2.5 Hip Trajectory

The hip trajectory is calculated via (4a) and (4b).

$$x_h(t) = \begin{cases} kD_s + x_{ed} & t = kT_c \\ (k+1)D_s - x_{sd} & t = kT_c + T_d \\ (k+1)D_s + x_{ed} & t = (k+1)T_c \end{cases} \quad (4a)$$

$$z_h(t) = \begin{cases} H_{h_{min}} & t = kT_c \\ H_{h_{max}} & t = kT_c + \frac{T_c - T_d}{2} \\ H_{h_{min}} & t = (k+1)T_c \end{cases} \quad (4b)$$

where $H_{h_{min}}$ and $H_{h_{max}}$ are the minimum and the maximum height of the hip, x_{ed} is the horizontal distance between the hip and the ankle's joint at the time of kT_c and x_{sd} is the horizontal distance between the hip and the ankle joint at the time of $kT_c + T_d$.

2.6 Inverse Kinematics

The kinematic parameters for the seven-links biped robot can be seen in Fig. 4. The ankle trajectory and hip trajectory are known and therefore, the related parameters of the inverse kinematics are calculated as (5), (6), (7) and (8).

$$l_f = \sqrt{(x_h - x_{af})^2 + (z_h - z_{af})^2} \quad (5)$$

$$\varphi_1 = \cos^{-1} \left(\frac{l_1^2 + l_f^2 - l_2^2}{2l_1 l_f} \right) \quad (6)$$

$$\varphi_2 = \cos^{-1} \left(\frac{l_2^2 + l_f^2 - l_1^2}{2l_2 l_f} \right) \quad (7)$$

$$\gamma = \cos^{-1} \left(\frac{x_h - x_{af}}{l_f} \right) \quad (8)$$

where, l_f , φ_1 and γ are shown in Fig. 4.

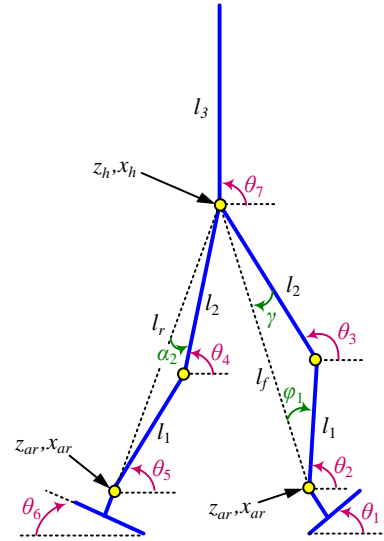


Fig. 4. Parameters of a seven-links biped robot

Equations (9) and (10) are the left shank and thigh angles.

$$\theta_2 = \gamma + \varphi_1 \quad (9)$$

$$\theta_3 = \gamma + \varphi_2 \quad (10)$$

Moreover, using the similar manner, the related parameters of the right shank and right thigh angles are obtained by (11), (12), (13) and (14).

$$l_r = \sqrt{(x_h - x_{ar})^2 + (z_h - z_{ar})^2} \quad (11)$$

$$\alpha_1 = \cos^{-1} \left(\frac{l_1^2 + l_r^2 - l_2^2}{2l_1l_r} \right) \quad (12)$$

$$\alpha_2 = \cos^{-1} \left(\frac{l_2^2 + l_r^2 - l_1^2}{2l_2l_r} \right) \quad (13)$$

$$\beta = \cos^{-1} \left(\frac{x_h - x_{ar}}{l_r} \right) \quad (14)$$

By using (12), (13) and (14), the right shank and thigh angles are obtained as

$$\theta_5 = \beta - \alpha_1 \quad (15)$$

$$\theta_4 = \beta + \alpha_2 \quad (16)$$

This should be highlighted that angles α_1 and φ_2 which are calculated via (13) and (8) was infeasible to be shown in Fig. 4.

3 Kinematic Modeling for the Biped Robot With Arms and Forearms

The kinematic parameters for the eleven-links biped robot is shown in Fig. 5. This figure represents the improvement of Fig. 3 by adding arms and forearms.

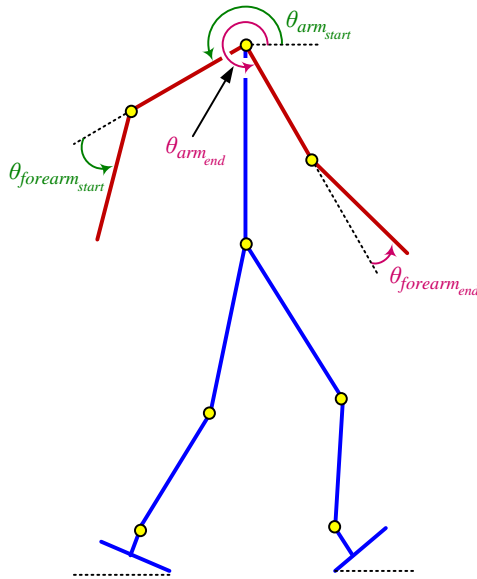


Fig. 5. Parameters of the improved eleven-links biped robot

Therefore, all position vectors and related angles can be obtained from Fig. 5. Position vectors for the sake of brevity are given in the Appendix.

4 Simulation

In this section, in the first step, the simulation is performed for the seven-links biped robot which was introduced in section 2. After that, in the second step, by adding arms and forearms, the eleven-links biped robot which was introduced in section 3 is simulated. The procedure of calculation for the eleven-links biped robot's simulation was figured out, based on the proposed algorithm for gait generation, in a humanoid robot with arms

and forearms. The flow chart of this algorithm is presented in Fig. 6.

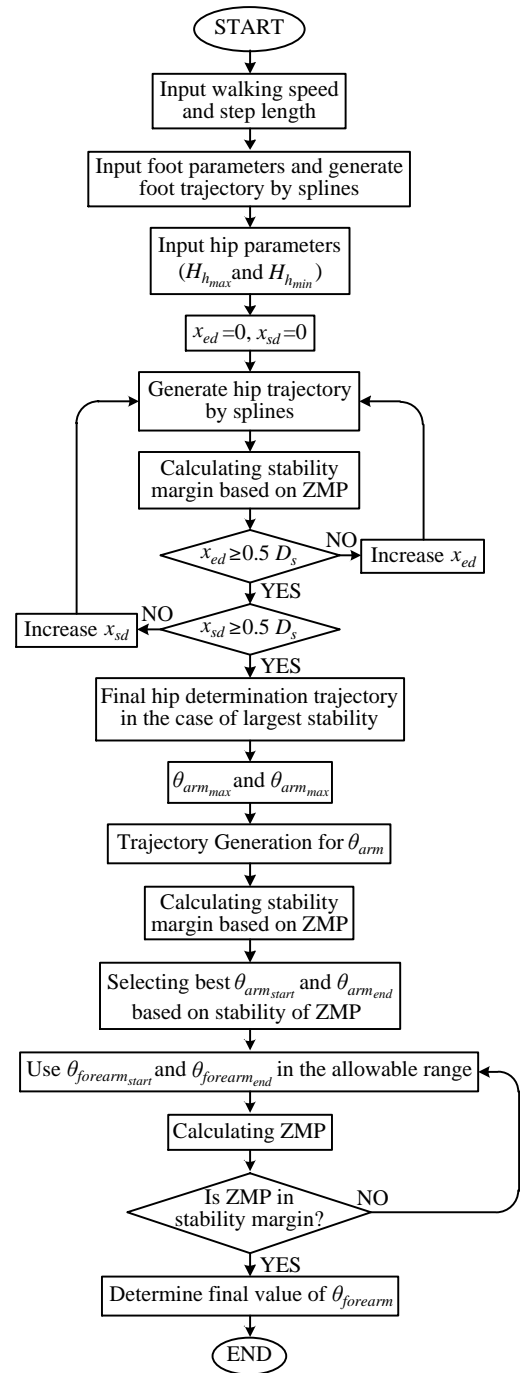


Fig. 6. Flowchart of the eleven-links biped robot's program

A point on the ground that the summation of all moments around it, is zero, called the zero moment point (ZMP). This point can be calculated via (17).

$$x_{ZMP} = \frac{\Gamma_1 - \Gamma_2 + \Gamma_3}{\psi} \quad (17)$$

where Γ_1 , Γ_2 , Γ_3 and ψ can be calculated from (18a), (18b), (18c) and (18d).

$$\Gamma_1 = \sum_{i=1}^n m_i (g \cos \lambda + \ddot{z}_i) x_i \quad (18a)$$

$$\Gamma_2 = \sum_{i=1}^n m_i (g \sin \lambda + \ddot{x}_i) z_i \quad (18b)$$

$$\Gamma_3 = \sum_{i=1}^n I \ddot{\theta}_i \quad (18c)$$

$$\psi = \sum_{i=1}^n m_i (g \cos \lambda + \ddot{z}_i) \quad (18d)$$

where g is the gravity acceleration, m_i is the mass of the link i , λ is the surface slope and in this study its value is zero, I_i is the inertia of the link i , \ddot{x}_i is the horizontal acceleration for the central mass of the link i , x_i is the horizontal position of the link i , \ddot{z}_i is the vertical acceleration for the central mass of the link i , z_i is the vertical position of the link i and $\ddot{\theta}_i$ is the angular acceleration of the link i .

If the ZMP remains in the polygon of the supporting legs, then the walking is stable. In order to accomplish a stable walking, there are some important parameters that should be considered. Regarding hip trajectory, it is observable that x_{sd} and x_{ed} have important roles in the trajectory of the hip joints. For each value of x_{sd} and x_{ed} , a distinct hip trajectory is obtained. Considering these conditions, we have:

$$0 \leq x_{sd} \leq 0.5D_s \quad (19a)$$

$$0 \leq x_{ed} \leq 0.5D_s \quad (19b)$$

By dividing the first above distance into n equal parts (the number of n is arbitrary), n values for x_{sd} are obtained. Using a similar manner, and by dividing the second distance into m equal parts (the number of m is also arbitrary), m values for x_{ed} are obtained. Thus, for each value of x_{sd} , it is possible to select m values of x_{ed} . Therefore, the number of cases will be $n \times m$ that for each set of x_{ZMP} can be calculated. However, it is important to select proper values of x_{sd} and x_{ed} . By iteration and choosing different values for x_{sd} and x_{ed} , the number of total iteration (NTI) is obtained as (20).

$$NTI = n \times m \quad (20)$$

Another factor that plays an important role in walking is T_m that its boundary condition is defined as $0.37 T_c \leq T_m \leq 0.41 T_c$. By dividing this time, into p equal parts, then, p values for T_m are obtained. Therefore, the number of total iteration increases and it is obtained as (21).

$$NTI = n \times m \times p \quad (21)$$

By adding more links, such as arms and forearms, the calculations are becoming more complex and time consuming. In order to tackle this issue, a step by step method is proposed. It is an algorithm to choose the suitable values in ZMP (i.e. x_{sd} and x_{ed}) for the eleven-links biped robot, using the previous parameters of the seven-links model. In this algorithm, by adding two more links (i.e. arms) to the seven-links model, the number of biped robot can be reached to nine-links. In this model,

$\theta_{arm_{start}}$ is the angle between x axes and arm at the beginning of the walking cycle and $\theta_{arm_{end}}$ is this angle at the end of the step. Furthermore, $\theta_{forearm_{start}}$ is the relative angle between arm and forearm at the start of walking cycle and $\theta_{forearm_{end}}$ is the relative angle between arm and forearm at the end of the step. Based on the $\theta_{arm_{start}}$ (i.e. θ_{arm} at $t = 0$), specifying $-\frac{\pi}{3} \leq \theta_{arm} \leq \frac{\pi}{3}$ and dividing this interval into q equal parts, then, q values for $\theta_{arm_{start}}$ are obtained. Finding a suitable value for $\theta_{arm_{start}}$ based on the best ZMP is important. Hence,

$$NTI_n = NTI_o \times q, \quad (22)$$

where q is the number of iterations related to the arm. q defines subintervals between $\theta_{arm_{start}}$ and $\theta_{arm_{end}}$. In fact q is a number that divides this intervals to equal parts. Moreover, NTI_n and NTI_o are the new total iteration and old total iteration, respectively. In the presented simulation, the best $\theta_{arm_{start}}$ was $-\frac{\pi}{3}$ (natural walking). By utilizing previous values of x_{sd} , x_{ed} and T_m , the new ZMP is calculated.

Considering ZMP calculations, after adding k -links to the robot (k is the number of added links to the robot) with n more links, the number of links reaches to $n + k$. The new ZMP is determined by using previous numerator and denominator of ZMP equation (17). However, it needs to be modified as (23).

$$x_{ZMP_{<n+k>}} = \frac{(\Gamma_1 - \Gamma_2 + \Gamma_3)_{<n>} + (\Gamma_1 - \Gamma_2 + \Gamma_3)_{<k>}}{\psi_{<n>} + \psi_{<k>}} \quad (23)$$

This new ZMP is estimated by using previous numerators and denominators of ZMP. Therefore, in this new model, the number of iterations are added by the only iterations of new parameters.

The simulated robot parameters and their specifications are shown in Table 1. In this table, q_b and q_f are the lift and the contact angles between the foot and the ground, D_s is the step length which is shown in Fig. 1, T_c is the total time (single support and double support times), T_d is the time of the double support phase, T_m is time that the ankle reaches to its maximum height, q_{gf} and q_{gs} are the ground initial terrain angles; and l_{ab} , l_{af} and l_{an} are lengths of related links in the foot and their related links are illustrated in Fig. 3. Moreover, l_{ao} is the horizontal distance between the ankle joint at the maximum height and the start point, l_{sh} is the length of the shank's link, l_{ti} is the length of the thigh's link, l_{arm} is the length of the arm's link, h_{min} and h_{max} are the minimum and maximum height of the hip's joint, m_{ankle} is the mass of ankle, I_{ankle} is the inertia of ankle, $\theta_{arm_{end}}$ is the angle between x axes and the arm's link at the end of the step, $\theta_{arm_{start}}$ is the angle between x axes and the arm's link at the start of the step, $l_{forearm}$ is the length of the forearm's link, $m_{forearm}$ is the mass of the forearm's link, $I_{forearm}$ is the inertia of the forearm, $\frac{forearm_{end}}{arm_{end}}$ is the relative angle between the arm and the forearm at the end of the step and $\frac{forearm_{start}}{arm_{start}}$ is the relative angle between the arm and the forearm at the start of the step.

Table 1. Simulated robot parameters and specifications

	l	H	D	m	q	θ	T	I
	[m]	[m]	[m]	[kg]	[deg]	[deg]	[s]	
b					12			
c							0.90	
d							0.18	
f					12			
s			0.5					
m							0.40	
gf					0			
gs					0			
ab	0.10							
af	0.13							
an	0.10							
ao	0.40	0.16						
sh	0.30			5.7				0.02
ti	0.30			10				0.08
tor	0.32			43				1.40
arm	0.20			3				0.02
h_{min}	0.60							
h_{max}	0.62							
$ankle$				3.3				0.01
arm_{end}						300		
arm_{start}						240		
$forearm$	0.02			2				0.01
$forearm_{end}$						0		
arm_{end}						45		
$forearm_{start}$								
arm_{start}								

5 Results and Discussions

5.1 Linear Velocities and Accelerations

The linear velocities of the robot's ankle and shank components are shown in Fig. 7 as the results of the simulation.

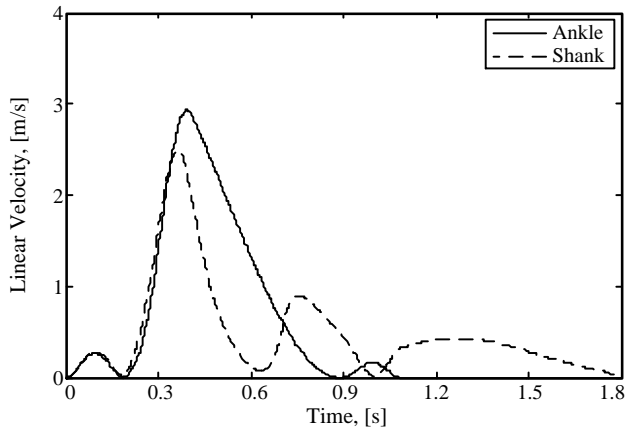


Fig. 7. Linear velocities of ankle and shank

Results in Fig. 7 are showing that the linear velocities of ankle and shank in their value are not huge. Moreover, velocity curves are rough. Therefore, it causes a smooth walking. Furthermore, the velocity of landing foot is zero and this prevents robot from destructive impact with the ground.

Figure 8 shows the linear velocities for the hip and the arm of the simulated eleven-links biped robot, during 1.8 seconds of its walking process. Based of the results which are presented in thid figure, the liner velocities of the hip and the arm are smooth. Hence, the robot has a smooth movement in its hip and arm.

Moreover, results which are yielded from simulation of the linear accelerations for the hip and shank of the eleven-links robot are shown in Fig. 9. This can be ob-

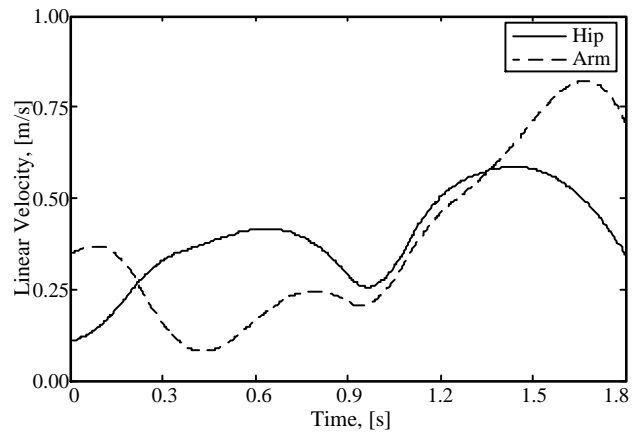


Fig. 8. Linear velocities of hip and arm

served that the linear accelerations of the hip and the shank are continuous and smooth. Therefore, it prevents the robot from the jerk related damages. Additionally, the linear acceleration of the supporting ankle at its related time is zero and this can be noticed. The linear acceleration of the shank during supporting phase is also approximately about zero. This is because of that the supporting foot does not move horizontally (it only swings in this phase). As a result of its swing during support phase, only small acceleration values are generated.

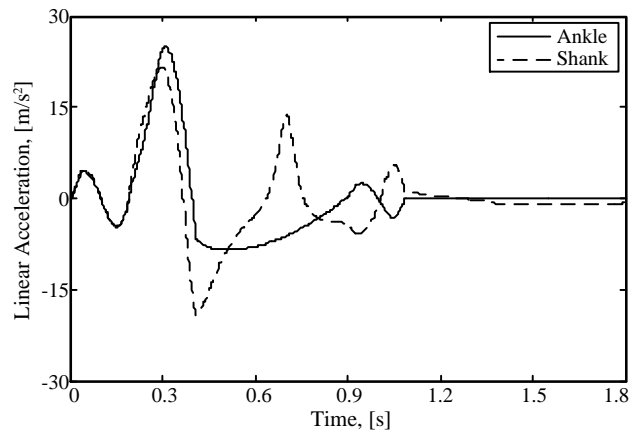


Fig. 9. Linear accelerations of ankle and shank

Results of simulation for the hip and the arm's linear accelerations of the eleven-links robot are exhibited in Fig. 10.

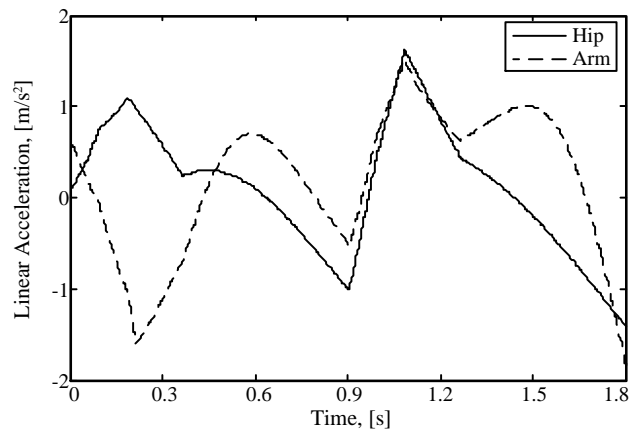


Fig. 10. Linear accelerations of hip and arm

Here, in Fig. 10, the linear accelerations of the hip

and the arm are not big. Thus, huge values of the destructive forces cannot occur on the simulated robot's joints. Ultimately, in all presented results of the simulation in Fig. 7, Fig. 8, Fig. 9 and Fig. 10, a smooth and acceptable behavior is observed.

5.2 Angular Velocities and Accelerations

Figure 11 shows the angular velocities of the ankle, the shank and the thigh of the simulated eleven-links biped robot. As a result, it is found that the angular velocities of the ankle, the shank and the thigh are smooth. It should be noted that during the supporting phase, the supporting foot does not rotate. Therefore, its joint (ankle) does not have angular velocity and its value is zero.

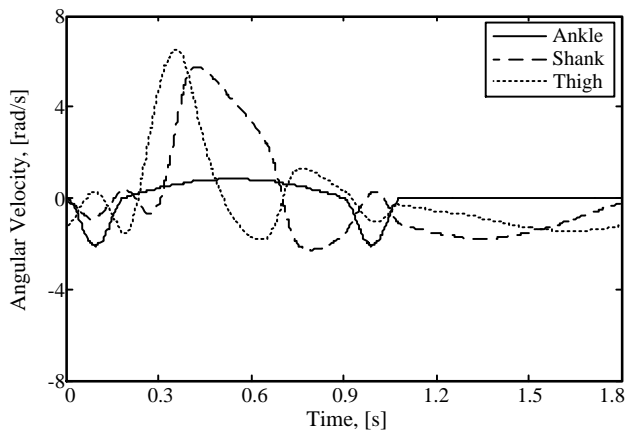


Fig. 11. Angular velocities of ankle, shank and thigh

The angular velocities of arms and forearms of the simulated eleven-links biped robot are presented in Fig. 12. The results show that the angular velocities of the arm and the forearm are smooth and continuous. Moreover, during the walking activity, the arm and the forearm have a rough swing.

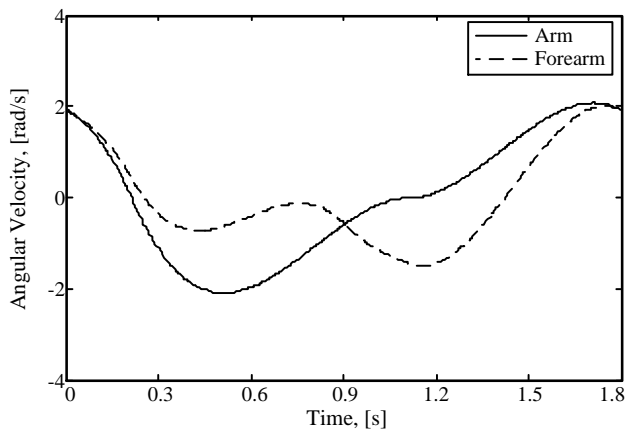


Fig. 12. Angular velocities of arm and forearm

In addition, the angular accelerations of the ankle, the shank and the thigh of the simulated eleven-links biped robot are demonstrated in Fig. 13. Based on these results, it is found that the angular acceleration is small at the supporting phase.

The angular accelerations of the robot's arm and the forearm are presented in Fig. 14. This is observed that the angular accelerations in terms of values are almost similar in some extents. However, the forearm has a more angular acceleration. This may be due to the fact that it

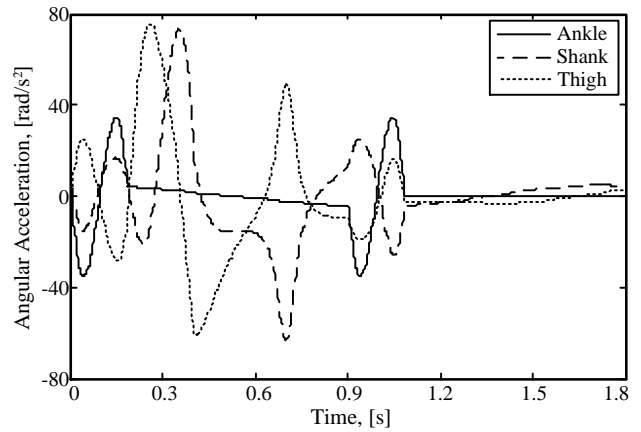


Fig. 13. Angular accelerations of ankle, shank and thigh is attached to the arm.

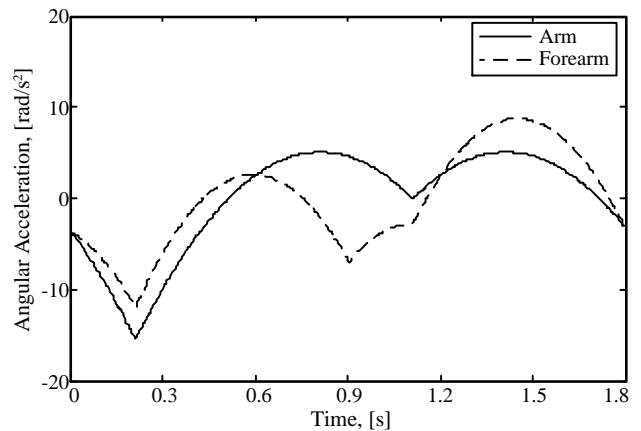


Fig. 14. Angular accelerations of arm and forearm

5.3 The robot's performances

The result of simulation for the eleven-links biped robot movement, which was presented in Fig. 5, is illustrated in Fig. 15. In other words, this figure is showing the stick diagram for walking of the simulated eleven-links biped robot. It shows that the robot is walking and during its walking cycle, the arm and the forearm have a rotation around their joints.

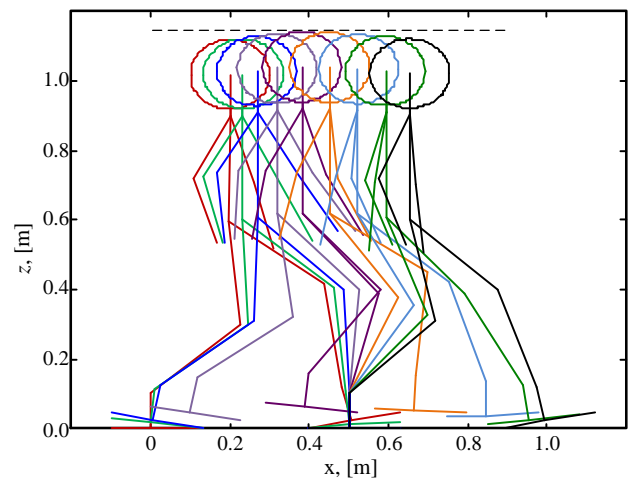


Fig. 15. The stick diagram for walking of the simulated eleven-links biped robot

The moving types of the ZMP for the simulated robot without arms (seven-links), with arms (nine-links) and

with forearms (eleven-links), when the robot moves in the distance of D_s are shown in Fig. 16. The blue and the red color lines in this figure are showing the ZMP margins; and the green line in the middle is the mean stability line. These lines are obtained based on the polygon of supporting legs in walking. Moreover, the smallest dashed line shows the ZMP with forearm, which is the best ZMP for this eleven-links biped robot.

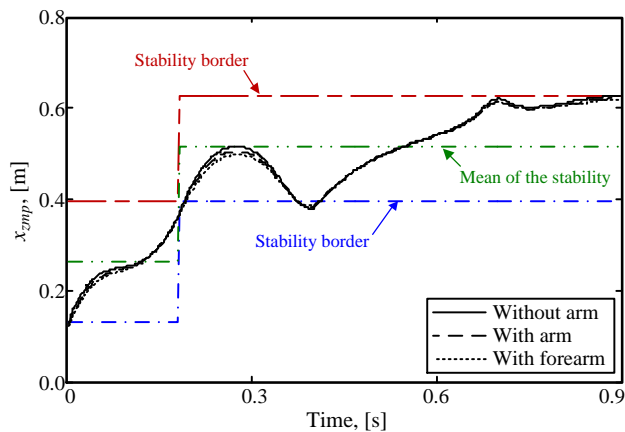


Fig. 16. Moving types of the robot's ZMP without arm, with arm and with forearm

In addition, the best ZMP is the one that is nearest to the mean stability border. It is because of that the ZMP should not be out of the acceptable borders, but it should be between the stability borders. Therefore, in order to select the best ZMP, the distance between each point of the curve and the middle horizontal line (green line) should be minimum. Consequently, this is because of that the middle horizontal line (mean of the stability) is far from the stability margins. By adding arms, the stability of the robot increases in comparison with the robot without arms. Besides, the robot with forearms has more stability in comparison with the robot with arms. Finally, by summation of all distances, it is also found that the ZMP of the robot with forearm is the best one.

6 Conclusion

A fast method for calculating trajectory of the eleven-links biped robot is developed based on the adjustment of new important parameters, which are obtained from the former studied seven-links biped robot. It is found that by applying the suggested method for the iteration, it is not required to use a huge number of repeats. As a result, the new ZMP can be quickly calculated. This method was used for humanoid robots by adding arms and forearms and it was able to achieve an acceptable stability for the robot's ZMP. Therefore, the pattern of walking for the robot and the swinging of the arm and the forearm are like human walking patterns. Results of the simulated method have shown that adding arms can rise the stability of the nine-links robot in comparison with the robot without arms (seven-links). Furthermore, it is found that the robot with forearms (eleven-links) has more stability in comparison with the robot with arms (nine-links).

REFERENCES

- [1] K. Hirai, M. Hirose, Y. Haikawa, and T. Takenaka, "The development of honda humanoid robot," in *Robotics and Automation, 1998. Proceedings. 1998 IEEE International Conference on*, vol. 2. IEEE, 1998, pp. 1321–1326.
- [2] M. Vukobratovic, A. A. Frank, and D. Juricic, "On the stability of biped locomotion," *Biomedical Engineering, IEEE Transactions on*, no. 1, pp. 25–36, 1970.
- [3] M. Yagi and V. Lumelsky, "Biped robot locomotion in scenes with unknown obstacles," in *Robotics and Automation, 1999. Proceedings. 1999 IEEE International Conference on*, vol. 1. IEEE, 1999, pp. 375–380.
- [4] M. J. Mahmoodabadi, M. Taherkhorsandi, and A. Bagheri, "Optimal robust sliding mode tracking control of a biped robot based on ingenious multi-objective PSO," *Neurocomputing*, vol. 124, pp. 194–209, 2014.
- [5] S. Bououden and F. Abdessemed, "Walking control for a planar biped robot using 0-flat normal form," *Robotics and Autonomous Systems*, vol. 62, no. 1, pp. 68–80, 2014.
- [6] Y. Farzaneh, A. Akbarzadeh, and A. A. Akbari, "Online bio-inspired trajectory generation of seven-link biped robot based on T-S fuzzy system," *Applied Soft Computing*, vol. 14, pp. 167–180, 2014.
- [7] Y. Aoustin and A. Hamon, "Human like trajectory generation for a biped robot with a four-bar linkage for the knees," *Robotics and Autonomous Systems*, vol. 61, no. 12, pp. 1717–1725, 2013.
- [8] T. McGeer, "Passive walking with knees," in *Robotics and Automation, 1990. Proceedings. 1990 IEEE International Conference on*. IEEE, 1990, pp. 1640–1645.
- [9] Y. F. Zheng and J. Shen, "Gait synthesis for the SD-2 biped robot to climb sloping surface," *Robotics and Automation, IEEE Transactions on*, vol. 6, no. 1, pp. 86–96, 1990.
- [10] A. Dasgupta and Y. Nakamura, "Making feasible walking motion of humanoid robots from human motion capture data," in *Robotics and Automation, 1999. Proceedings. 1999 IEEE International Conference on*, vol. 2. IEEE, 1999, pp. 1044–1049.
- [11] J. W. Grizzle, C. Chevallereau, R. W. Sinnet, and A. D. Ames, "Models, feedback control, and open problems of 3D bipedal robotic walking," *Automatica*, 2014.
- [12] H. Siswoyo Jo and N. Mir-Nasiri, "Dynamic modelling and walk simulation for a new four-degree-of-freedom parallelogram bipedal robot with sideways stability control," *Mathematical and Computer Modelling*, vol. 57, no. 1, pp. 254–269, 2013.
- [13] J. G. Juang, "Intelligent locomotion control on sloping surfaces," *Information Sciences*, vol. 147, no. 1, pp. 229–243, 2002.
- [14] C. Sabourin and O. Bruneau, "Robustness of the dynamic walk of a biped robot subjected to disturbing external forces by using CMAC neural networks," *Robotics and Autonomous Systems*, vol. 51, no. 2, pp. 81–99, 2005.
- [15] Y. Wu, Q. Song, and X. Yang, "Robust recurrent neural network control of biped robot," *Journal of Intelligent and Robotic Systems*, vol. 49, no. 2, pp. 151–169, 2007.
- [16] G. Capi, Y. Nasu, L. Barolli, and K. Mitobe, "Real time gait generation for autonomous humanoid robots: A case study for walking," *Robotics and Autonomous Systems*, vol. 42, no. 2, pp. 107–116, 2003.
- [17] S. Kajita, T. Nagasaki, K. Kaneko, K. Yokoi, and K. Tanie, "A hop towards running humanoid biped," in *Robotics and Automation, 2004. Proceedings. ICRA'04. 2004 IEEE International Conference on*, vol. 1. IEEE, 2004, pp. 629–635.
- [18] F. M. Silva and J. A. T. Machado, "Energy analysis during biped walking," in *Robotics and Automation, 1999. Proceedings. 1999 IEEE International Conference on*, vol. 1. IEEE, 1999, pp. 59–64.
- [19] S. L. Cardenas-Maciuel, O. Castillo, and L. T. Aguilar, "Generation of walking periodic motions for a biped robot via genetic algorithms," *Applied Soft Computing*, vol. 11, no. 8, pp. 5306–5314, 2011.
- [20] C. Pinto and A. P. Santos, "Modelling gait transition in two-legged animals," *Communications in Nonlinear Science and Numerical Simulation*, vol. 16, no. 12, pp. 4625–4631, 2011.
- [21] Q. Huang, K. Yokoi, S. Kajita, K. Kaneko, H. Arai, N. Koyachi, and K. Tanie, "Planning walking patterns for a biped robot," *Robotics and Automation, IEEE Transactions on*, vol. 17, no. 3, pp. 280–289, 2001.
- [22] P. N. Mousavi and A. Bagheri, "Mathematical simulation of a seven link biped robot on various surfaces and ZMP considerations," *Applied Mathematical Modelling*, vol. 31, no. 1, pp. 18–37, 2007.

Appendix

$$x_{knee,R} = x_{ankle,R} + l_1 \cos(\theta_5) \quad (24a)$$

$$z_{knee,R} = z_{ankle,R} + l_1 \sin(\theta_5) \quad (24b)$$

$$x_{knee,L} = x_{ankle,L} + l_1 \cos(\theta_2) \quad (24c)$$

$$z_{knee,L} = z_{ankle,L} + l_1 \cos(\theta_2) \quad (24d)$$

$$x_{hip} = x_{ankle,R} + l_1 \cos(\theta_2) + l_2 \cos(\theta_3) \quad (24e)$$

$$z_{hip} = z_{ankle,R} + l_1 \sin(\theta_2) + l_2 \sin(\theta_3) \quad (24f)$$

$$x_{tor} = x_{hip} + l_3 \cos(\theta_7) \quad (24g)$$

$$z_{tor} = z_{hip} + l_3 \sin(\theta_7) \quad (24h)$$

$$x_{elbow,R} = x_{tor} + l_{arm} \cos(\theta_{arm,R}) \quad (24i)$$

$$z_{elbow,R} = z_{tor} + l_{arm} \sin(\theta_{arm,R}) \quad (24j)$$

$$x_{elbow,L} = x_{tor} + l_{arm} \cos(\theta_{arm,L}) \quad (24k)$$

$$z_{elbow,L} = z_{tor} + l_{arm} \sin(\theta_{arm,L}) \quad (24l)$$

$$x_{wrist,R} = x_{elbow,R} + l_{forearm} \cos(\theta_{forearm,R}) \quad (24m)$$

$$z_{wrist,R} = z_{elbow,R} + l_{forearm} \sin(\theta_{forearm,R}) \quad (24n)$$

$$x_{wrist,L} = x_{elbow,L} + l_{forearm} \cos(\theta_{forearm,L}) \quad (24o)$$

$$z_{wrist,L} = z_{elbow,L} + l_{forearm} \sin(\theta_{forearm,L}) \quad (24p)$$